International Scholarly Research Network
ISRN Materials Science
Volume 2011, Article ID 718761, 10 pages
doi:10.5402/2011/718761

Review Article

Thermal Conductivity of High-Strength Polyethylene Fiber and Applications for Cryogenic Use

Atsuhiko Yamanaka[1] and Tomoaki Takao[2]

[1] *Research Center, Toyobo Co., Ltd., 2-1-1, Katata, Ohtsu, Shiga 520-0292, Japan*
[2] *Faculty of Science and Technology, Sophia University, 7-1, Kioi-Cho, Chiyoda-Ku, Tokyo 102-8554, Japan*

Correspondence should be addressed to Atsuhiko Yamanaka, atsuhiko_yamanaka@toyobo.jp

Received 6 July 2011; Accepted 25 July 2011

Academic Editors: C. Carbonaro and F. Herlach

The local temperature rise of the tape is one of instabilities of the conduction-cooled high temperature superconducting (HTS) coils. To prevent the HTS tape from locally raising a temperature, high thermal conductive fiber reinforced plastic was applied to coil bobbin or spacer for heat drain from HTS tape. The thermal conductivity of ramie fibers increases by increasing orientation of molecular chains with drawing in water, and decreases by chain scission with γ-rays irradiation or by bridge points in molecular chains with vapor-phase-formaldehyde treatments. Thermal conductivity of high strength ultra-high-molecular-weight (UHMW) polyethylene (PE) fiber increases lineally in proportion to tensile modulus and decreases by molecular chain scissions with γ-rays irradiation. This result suggested the contribution of the long extended molecular chains due to high molecular weight on the high thermal conductivity of high strength UHMW PE fiber. Thermal conductivity of high strength UHMW PE fiber reinforced plastics in parallel to fiber direction is proportional to the cross sectional ratio of reinforcement oriented in the conduction direction. Heat drain effect of high strength UHMW PE fiber reinforced plastic from HTS tape is higher than that of glass fiber reinforced plastic (GFRP) and lower than that of aluminum nitride (AlN). In the case of HTS coil, the thermal stability wound on coil bobbin made of high strength UHMW PE fiber reinforced plastic is good as that of AlN, and better than that of GFRP.

1. Introduction

In applications of polymeric materials, the thermal conductivity has been an important property, for example, for a cool/warm sensation for clothing fiber or wood product, or in the thermal insulation of plastics including styroforms [1–4]. With the recent development of superconducting and electronic engineering technologies, thermal conductivities of structural and insulating materials used as composites in cryogenic and heat-releasing materials in electrical equipment have become more important. Furthermore, the desired features vary, depending upon the application, from insulation for use in cryostat [5] to high-thermal conductivity for use in superconducting coils [6] and electronic engineering [7]. For example, the thermal conduction between a superconductor and the cold head of a refrigerator is important for the stability of a conduction-cooled superconducting coil, because this connection is the only heat-flow-pathway for cooling superconductor [8].

Thermal conductivities of most of polymer materials are lower than those of metals as shown in Figure 1. From previous studies of polymer materials, it is well-known that the thermal conductivities of amorphous polymers are smaller than those of metals and semiconductors [9, 10]. Therefore, these have principally been used as heat insulators. However, other reports have shown that polymeric crystals possess high thermal conductivity in the direction in which the molecular chains are covalently bonded, polyethylene crystals being an example [11, 12]. Thus, high-crystallized and high-oriented polymers exhibit high thermal conductivity [10–15]. For example, highly crystallized polymer materials including high-strength polyethylene (PE) fiber [15–18] and high-strength polypara-phenylene-benzo-bis-oxazole (PBO)

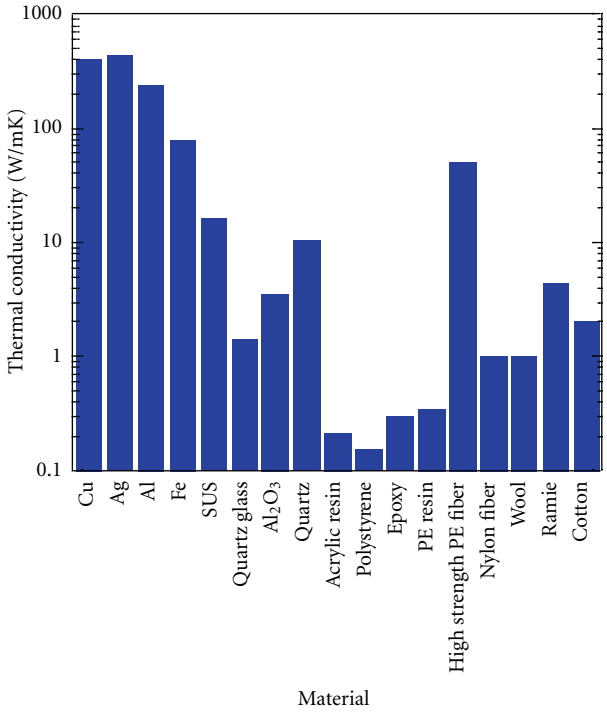

Figure 1: Thermal conductivities of industrial materials.

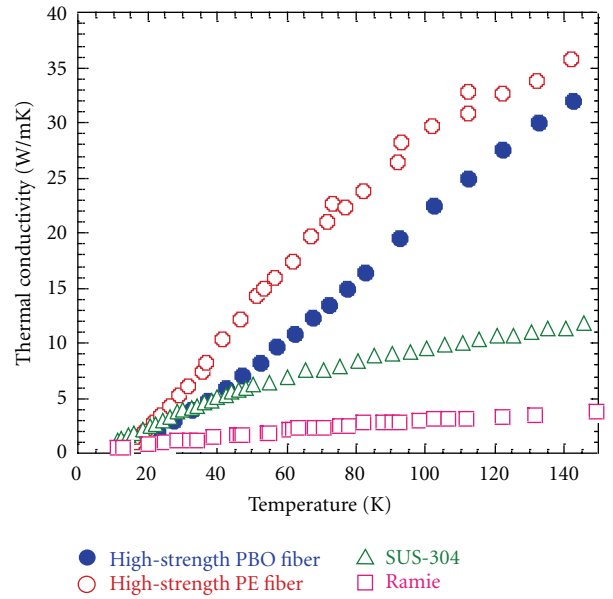

Figure 2: Thermal conductivities of high-thermal-conductive polymer fibers [18].

fiber [16] are known to possess high thermal conductivity similar to those of metals as shown in Figure 2. The high-strength PE fiber and PBO fiber shown in Figure 2 are Dyneema® SK-60 (hereinafter abbreviated to DF) and Zylon® HM (TOYOBO CO.) [18–20].

In this paper, we report the thermal conductivity of high-strength PE fiber and application of the high-strength PE fiber reinforced plastics for conduction-cooled high-temperature superconducting (HTS) coil.

2. Thermal Conductivity of High-Strength Polyethylene Fiber

2.1. Thermal Conductivity of Polymer Fiber. The thermal conductivity of solid, electrical insulating materials is introduced attributable to phonons [12, 13], and the heat in polymers is conducted in the direction of covalently bonded molecular chains, whereas conduction in the direction to intermolecular chains bonded by Van der Waals forces is much less. It is known that thermal conductivities of PE, polyethyleneterephtalate, and polypropylene toward to the direction of molecular chain increase by the increasing crystallinity and orientation of crystal [11, 13–17, 21, 22]. In the case of amorphous polymers, it is also known that thermal conductivities of polymethylmethacrylate and polystyrene increase by the orientation of molecular chain [16, 23, 24].

The thermal conductivity of solid electrically insulating materials is affected by the scattering of phonons. The phonon scattering is considered to be introduced by imperfections in the material. For example, crystal or amorphous boundary, defects, chemical bridge points, and the ends and entanglements of the molecular chains can scatter phonons and interfere with the thermal transmittance in polymer materials. Dependence of thermal conductivity on molecular weight has been reported about polystyrene film [25].

In the case of polymer fibers, the thermal conductivity in fiber direction depends on the crystallinity, orientation, crystal size, length of molecular chains, chemical bridge points, and morphologies composed of crystal and amorphous.

For example, thermal conductivity of ramie fiber in fiber direction changes by the following treatments, drawing in water (water treatment), irradiation with γ-rays (γ-rays treatment), and vapor-phase-formaldehyde treatments (VP-HCHO treatment). Those treatments induce the extension, chain scission, and bridging to molecular chains as shown in Figure 3 [26–28]. The thermal conductivities of the ramie fibers before and after those treatments are shown in Figure 4 [26–28].

It is reported that the tensile modulus is increased by the increasing of orientation degree of molecular chains in the amorphous region of ramie fiber by water treatment [31]. It is also known that tensile modulus of ramie fiber increases by water treatment [31]. Thermal conductivity of ramie fiber in the fiber direction increases by water treatment as shown in Figure 4 [26]. In this water treatment, ramie fibers were drawn by the stress of 17.4 kg/mm^2 in the water. The tensile modulus of the ramie fiber doubles by this water treatment. The increasing of thermal conductivity by water treatment is inferred to be caused by the extension of molecular chains in the amorphous region as shown in Figure 3 [26].

It is well known that fibers mainly made of cellulose, including ramie and cottons, undergo main chain scission by γ-rays treatment [32] as shown in Figure 3. And it is also known that the crystallinity is not decreased by irradiation

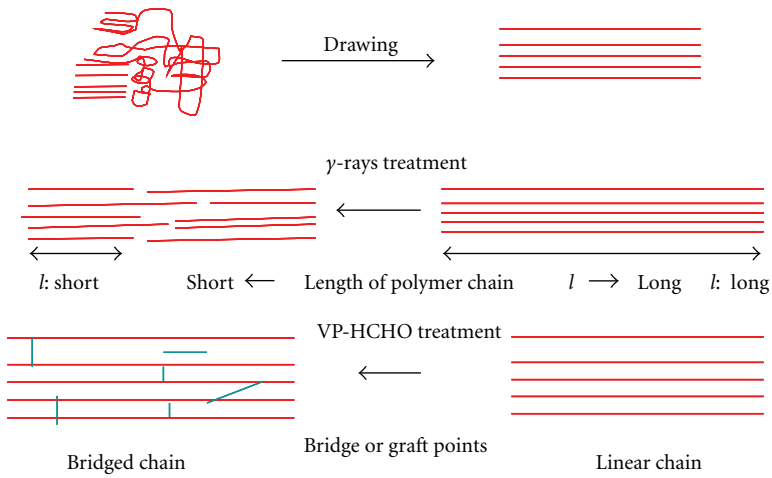

Figure 3: Schematic diagram of molecular chains of cellulose with drawing, γ-rays treatment, and VP-HCHO treatment.

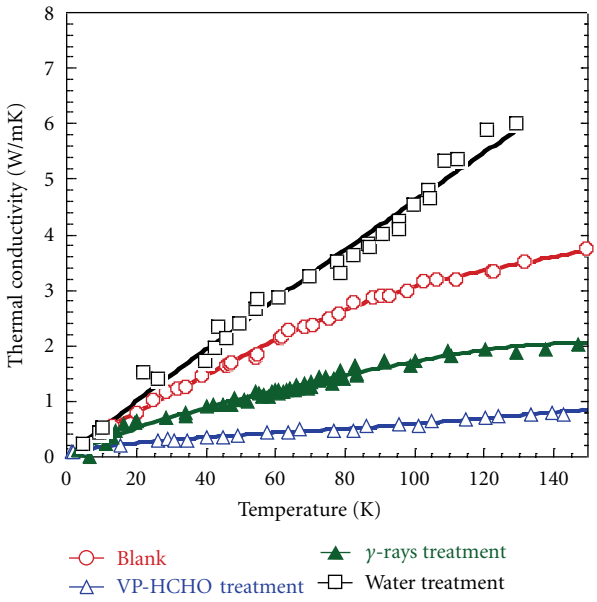

Figure 4: Thermal conductivities of ramie fibers with water treatment, g-rays treatment, and VP-HCHO treatment [26–28].

with γ-rays in the case of appropriate dose rate [27, 32]. Thermal conductivity of ramie fiber in fiber direction decreases by γ-rays treatment as shown in Figure 4 [27]. It is reported that the decreasing of thermal conductivity of ramie fiber by γ-rays treatment agrees to the decreasing of the degree of polymerization (DP) of ramie fibers. In this case, shown in Figure 4, the irradiation was carried out with Co-60 γ-rays and the total absorbed dose was 100 kGy [27]. The DP of ramie fibers decreases from 1700 to 220 by this γ-rays treatment. The decreasing of thermal conductivity by γ-rays treatment is inferred to be caused by molecular chain scission. That is to say, thermal conductivity of ramie fibers depends on the length of molecular chain [27].

Fibers mainly made of cellulose, including ramie and cottons, are well known for being bridged with formaldehyde (HCHO) [31, 37, 39–44], for example, by VP-HCHO treatment [39] as shown in Figure 3. This technology is employed for stabilizing the conformity of cellulose fibers and is used practically in clothing materials such as wash and wear shirts [40, 42–45]. Thermal conductivity decreases to about 20–25% by VP-HCHO treatments as shown in Figure 4 [28]. It is reported that the thermal conductivity decreases by increasing the concentration of bound HCHO [28]. In this case, shown in Figure 4, the concentration of bound HCHO of the VP-HCHO-treated ramie fiber was 1.6% [28]. The decreasing of thermal conductivity of ramie fiber by VP-HCHO treatment is inferred to be caused by scattering of phonon at bridge points combined with HCHO [28].

In this way, the thermal conductivity of ramie fibers increases by increasing orientation of molecular chains and decreases by chain scission or by bridge points in molecular chains [26–28]. That is to say that the thermal conductivities of polymer fibers depend on the structures, for example, orientation, length (molecular weight), and bridge points of molecular chains.

2.2. Thermal Conductivity of High-Strength Polyethylene Fiber

2.2.1. High Thermal-Conducting Polymer Fiber. As above mentioned, high-strength PE fiber has a high thermal conductivity in fiber direction [18–20]. DF shown in Figure 2 is one of the high-strength ultra-high-molecular-weight (UHMW) PE fibers made by gel spinning method [46–51]. In this section, the mechanism of high thermal conduction of DF is reported.

It is well known that the random-oriented crystal region composed of folding UHMWPE chains changes to highly oriented crystal region composed of extended chains by gel spinning as shown in Figure 5 [29, 46–51]. Therefore, it is considered that heat conduction of the extended chains in the direction covalent-bonded chain axis in crystal regions contributes to the high thermal conductivity of DF [18–20].

The relationship between the thermal conductivity and the structure of DF is reported in the following.

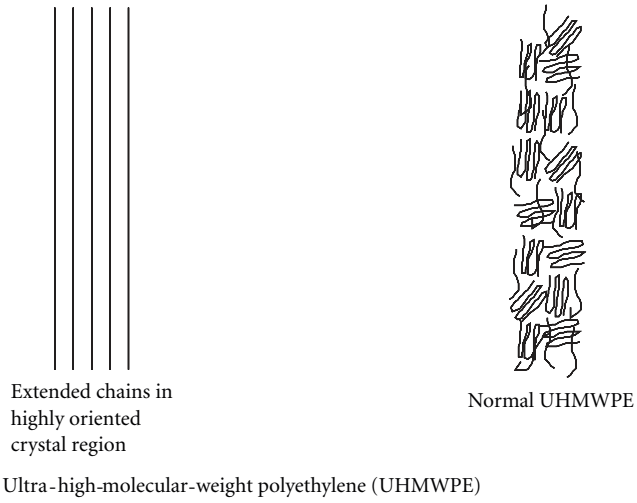

Figure 5: Schematic diagram of molecular chains in UHMW-PE [29].

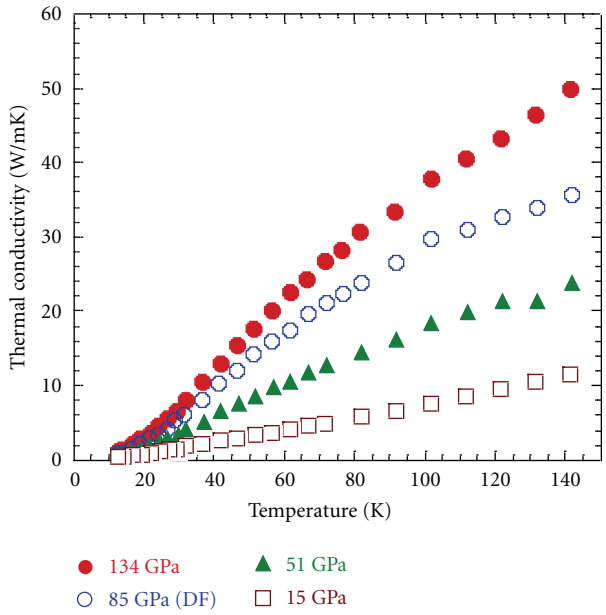

Figure 6: Thermal conductivities of high-strength PE fibers having different modulus [20].

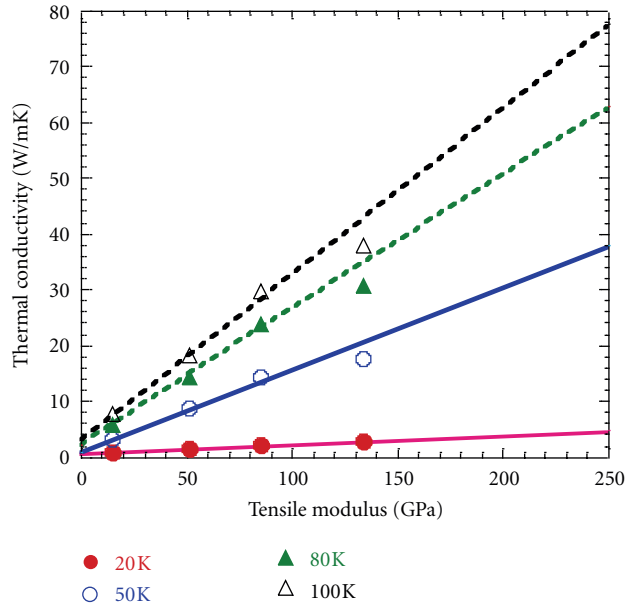

Figure 7: Relationship between the thermal conductivities and tensile module of high-strength PE fibers.

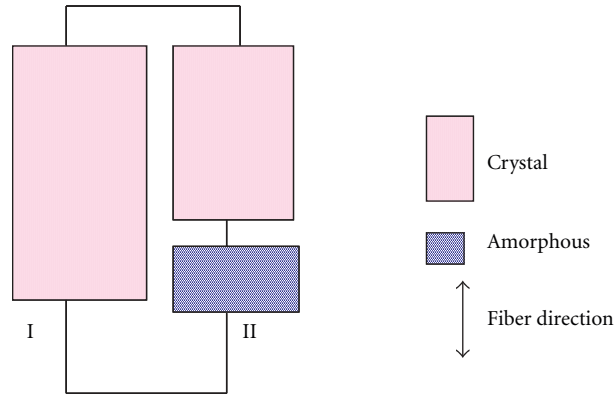

I: Continuous crystal part composed of extended molecular chains

II: Series combination part of crystal and amorphous

Figure 8: Schematic diagram showing the structure of high-strength PE fiber by mechanical model [20].

2.2.2. Dependence of Thermal Conductivity on Tensile Modulus of High-Strength Polyethylene Fiber [20]. Thermal conductivities of high-strength UHMW PE fibers (hereinafter abbreviated to PEFs) made by gel spinning method with different draw ratios are shown in Figure 6 [20]. They have different modulus shown as follows: A: 15 GPa, B: 51G Pa, C(DF): 85 GPa, and D: 134 GPa. Thermal conductivity increases with increasing tensile modulus of PEF, and all of them increase with increasing temperature as shown in Figure 6. The relations between thermal conductivity and tensile modulus of the PEFs are shown in Figure 7. Thermal conductivity of PEFs increases lineally in proportion to tensile modulus.

The relationship between the thermal conductivities and tensile modulus of PEFs was explained by the fiber structure illustrated in the mechanical serial-parallel model (Takayanagi model), which consists of a crystalline/amorphous structure as shown in Figure 8 [20]. This mechanical model is composed of the following two parts by parallel combination. One of them is continuous crystal part composed of extended molecular chains, and the other is series combination part of crystal and amorphous. In this mechanical model composed of continuous crystal region and series combination part composed of crystal and amorphous, thermal conductivity of the PEF in fiber

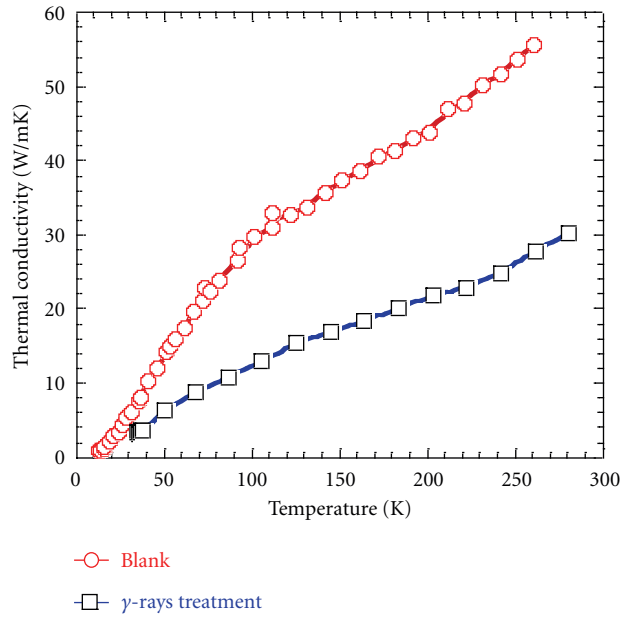

Figure 9: Thermal conductivity of high-strength PE fiber with γ-rays treatment [30].

direction is dominated by that of continuous crystal region composed of extended molecular chains [20].

2.2.3. Radiation Effect on Thermal Conductivity of High-Strength Polyethylene Fiber by γ-Ray [30]. The contribution to thermal conductivity by the length of the molecular chains in high-strength PEF is reported in this section. It is known that polyethylene undergoes main chain scission by irradiation with γ-rays (γ-rays treatment) in the presence of oxygen [52].

Thermal conductivities of PEFs with γ-rays treatments are shown in Figure 9 [30]. The used PEF was DF. Irradiation was carried out with Co-60 γ-rays, and the total absorbed dose was 0.5 MGy; that is hereinafter abbreviated to DF (γ-rays treatment). The DF without γ-rays treatment is abbreviated to DF (Blank). Thermal conductivity of DF decreases to 50% by γ-rays treatment at every temperature [30].

The measured molecular weight of DF (Blank) was 2.0×10^6. It decreased to 2.6×10^4 by 0.5 MGy irradiation. This result shows the main chain scission of DF by the γ-rays treatment. On the other hand, the change of the crystal structure of DF by γ-rays treatment could not be observed. Therefore, the decrease of thermal conductivity of DF by γ-rays treatment was explained by the molecular main chain scission as similar to the case of ramie described in the above mentioned. This result suggested the contribution of the length of extended molecular chains due to high molecular weight on the thermal conductivity of DF [30].

2.2.4. Summary. With aforementioned, high-strength PE fiber has a high thermal conductivity in fiber direction, and this high thermal conductivity is explained by the

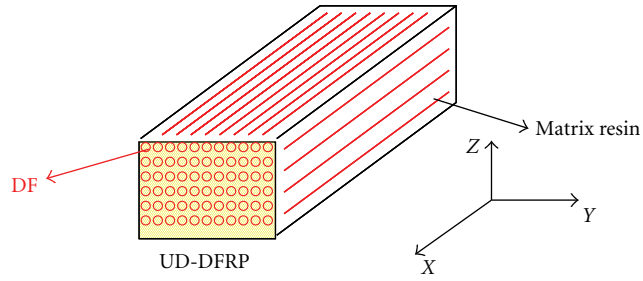

Figure 10: Schematic diagram of UD-DFRP.

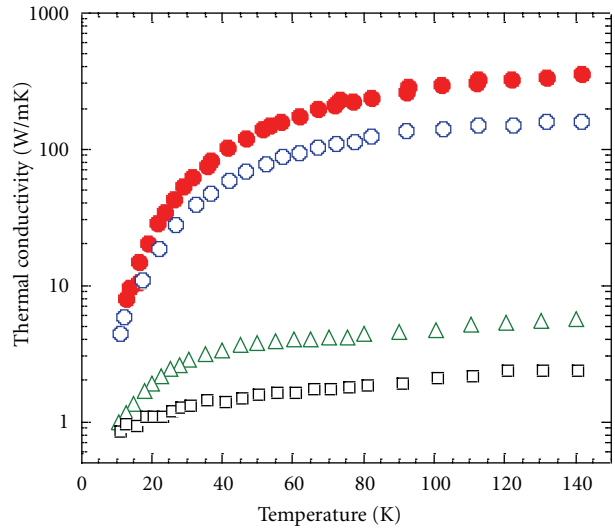

Figure 11: Thermal conductivities of DF and DFRP [18]. •: DF in parallel to the fiber direction, ◯: DFRP in parallel to the fiber direction, △: DFRP in perpendicular to the fiber direction, □: Epoxy.

mechanical series-parallel model composed of crystal and amorphous including continuous crystal region composed of long extended molecular chains [20, 30].

2.3. Thermal Conductivity of High-Strength Polyethylene Fiber Reinforced Plastics [18, 53]. In order to apply the PEFs to the cryogenic use, for example, coil bobbin or spacer of superconducting coils, thermal conductivities of PEF-reinforced plastics are important as described in the following sections. In this section, the PEF used as the reinforcement is DF. Hereinafter, DF-reinforced plastics is abbreviated to DFRP. The schematic diagram of unidirectional (UD) DFRP is shown in Figure 10.

Thermal conductivities of UD-DFRP in parallel and perpendicular to fiber direction are shown in Figure 11 [18]. Thermal conductivity of DFRP in parallel to fiber direction shows about medium value between those of DF and epoxy resin. Dependence of thermal conductivity on volume fraction (Vf) of DF in UD-DFRP is shown in Figure 12. Thermal conductivity of UD-DFRP is proportional to Vf of DF as shown in Figure 12 [18]. Therefore, thermal conductivity of DFRP in parallel to fiber direction is proportional to

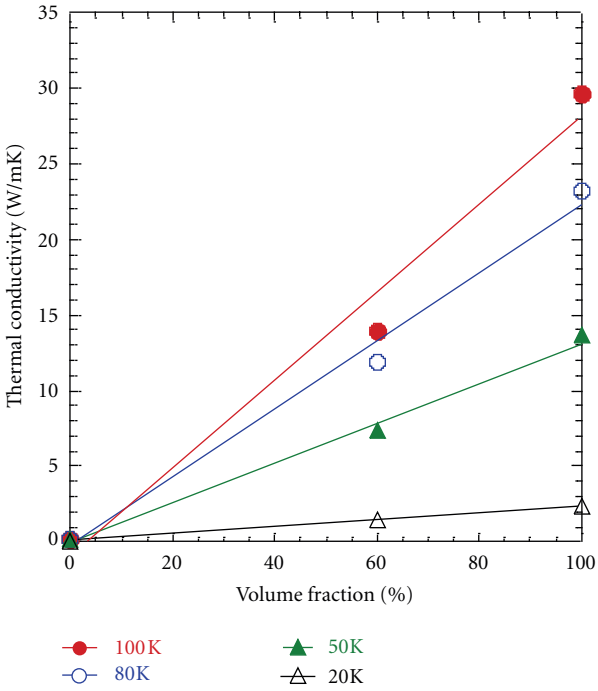

Figure 12: Vf dependence of thermal conductivity of UD-DFRP on fiber direction.

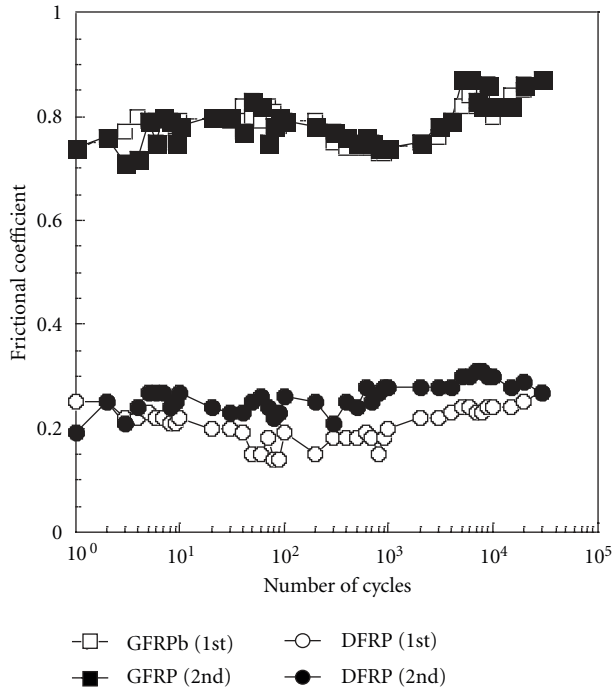

Figure 13: Frictional coefficients of DFRPs and GFRPs [33].

the cross-sectional ratio of DF oriented in the conduction direction [18].

Thermal conductivity of UD-DFRP in the perpendicular to fiber direction is one order magnitude smaller than that in the parallel to fiber direction [18].

It is known that the thermal conductivity of hybrid FRP including DF can be expressed by the law of mixtures [53].

3. Application of High-Strength Polyethylene-Fiber-Reinforced Plastics for Conduction-Cooled High-Temperature Superconducting Coil

3.1. Instability of HTS Coil by Local Temperature Rise of HTS Tape. When the cooling power of a refrigerator exceeds the loss in HTS coil and conduction heat along the current leads, steady state operation of conduction-cooled coil is possible [54]. However, if a cooling condition of the HTS tape in the coil is partly insufficient, a local hot spot occurs in the conduction-cooled coil during operation of the coil [55]. The local temperature rise of the tape is one of instabilities of the conduction-cooled HTS coils. To prevent the HTS tape from locally raising a temperature, it is necessary to drain heat from HTS tape to electrical insulation materials in the coil effectively. For effective heat drain from HTS tape to electrical insulation materials, high-thermal-conduction electrical insulator is necessary for coil bobbin or spacer [6].

Usually, glass-fiber-(GF-) reinforced plastics (GFRP) were used as electrical insulation materials for HTS coil, for example, coil bobbin or spacer. However, GFRP is a thermal insulator. Therefore, heat drain from HTS tape to GFRP is insufficient. On the other hand, aluminum nitride (AlN) is known as an electrical insulator and a thermal conductor. However, the AlN is hard and brittle, and, hence, difficult for coil makers and users to process the electrical insulation parts in the coil, for example, spacers [6].

In the following sections, effect of heat drain of PEF-reinforced plastics for electrical insulation material of HTS coils is reported. DFRP reinforced plastic is used as a PEF-reinforced plastic in the following sections.

3.2. Important Physical Properties of High-Strength Polyethylene-Fiber-Reinforced Plastics for HTS Coil. Important physical properties of DFRP except for thermal conductivity are reported in this section in order to report the HTS coils in the following sections. Frictional coefficients, surface spark voltages, and thermal contraction by cooling of DFRP are shown in Figures 13, 14 and 15. DFRP has a lower frictional coefficient and higher spark voltage than those of GFRP [33, 34]. DFRP has a negative thermal expansion coefficient in fiber direction [35, 36]. Therefore, DFRP expands in fiber direction by cooling down from room temperature to liquid nitrogen temperature as shown in Figure 15 [35, 36].

3.3. Heat Drain Effects from HTS Tapes to High-Strength Polyethylene-Fiber-Reinforced Plastics [38]. In this section, the heat drain effect of the DFRP with a steady-state current to the HTS tape is reported. The schematic illustration of experimental arrangement is shown in Figure 16. Bi-2223 is used as a HTS tape in this section. DFRP, GFRP, and AlN were used as structural materials in Figure 16. Volume fraction of fiber of DFRP and GFRP were 50% (hereinafter abbreviated to DFRP-50 and GFRP-50). The structural

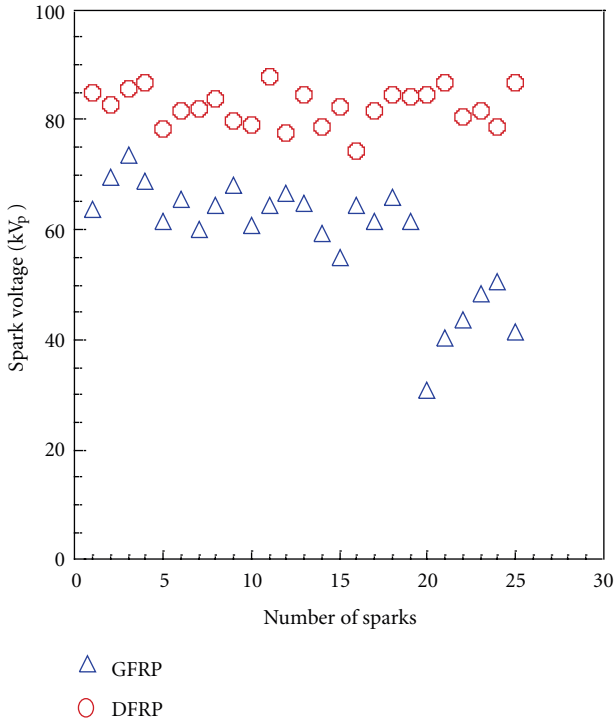

Figure 14: Surface spark voltage in Liq. He [34].

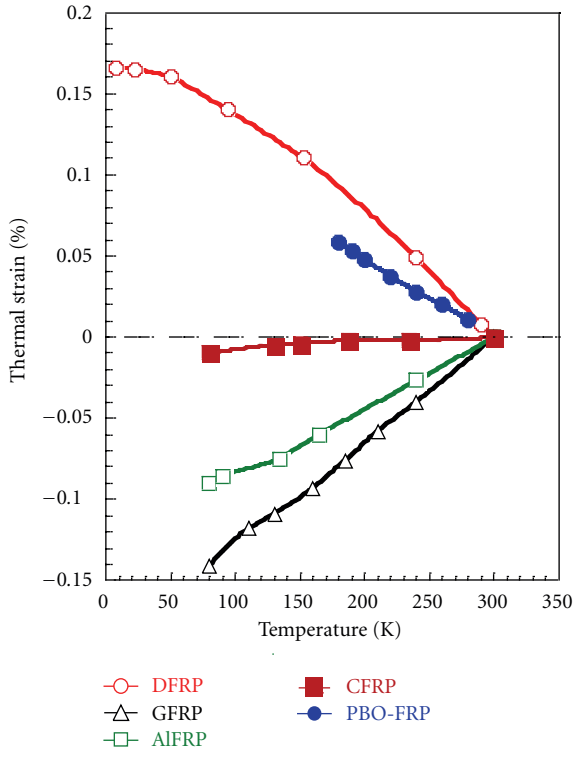

Figure 15: Thermal strain of UD-FRP in fiber direction by cooling down [35, 36].

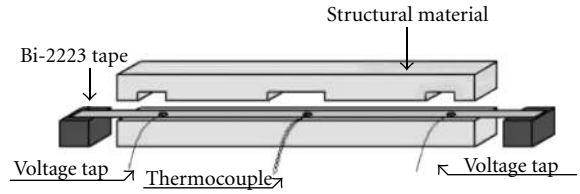

Figure 16: The schematic illustration of experimental arrangement [37].

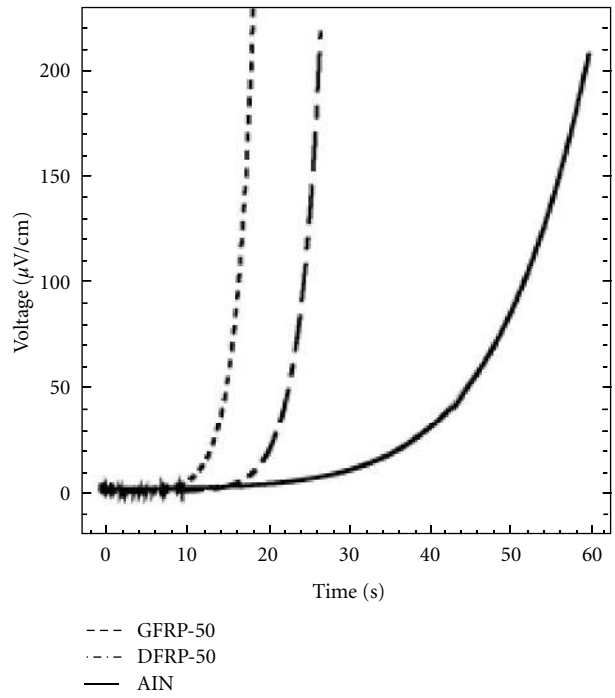

Figure 17: The voltages of the tap clamped by GFRP-50, DFRP-50, and AlN [38].

Table 1: Specifications of Bi-2223 tape and clamping materials.

	Bi2223 tape	Clamping materials
Width (mm)	4.1	9
Thickness (mm)	0.21	9
Length (mm)	150	124
Ag ratio	2.2	
Ic at 77 K	60 A	
Material	Ag, Bi-2223	DFRP, GFRP, AlN

materials were used as clamping materials. Specifications of the clamping materials and the Bi tape are listed in Table 1. The set of the clamping materials, the clamped tape, and the weight is on a cold head of a refrigerator and is cooled down to 77 K. A steady current of 60 A, which equaled to the critical current of the Bi tape, was applied to the tape, and the voltage between the tapes was observed [38].

The voltages of the tape clamped by GFRP-50, DFRP-50, and AlN are shown in Figure 17. As shown in Figure 18, when the clamping material is the AlN, the voltage keeps

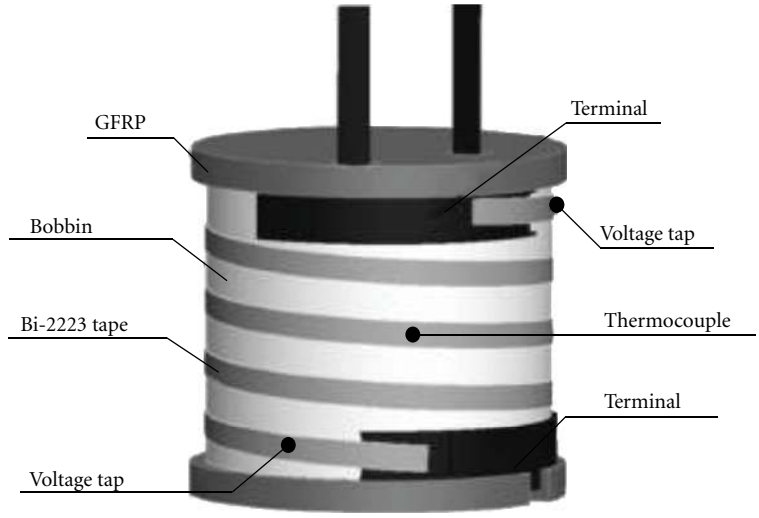

Figure 18: Schematic illustration of HTS coil [8].

relatively low, that is to say, the temperature rise of the tape is very slow [38]. On the contrary, the voltage of the GFRP-50 took off within a short time from the current start, and the temperature rise of the tape was fast [38]. DFRP-50 shows the middle behavior between GFRP-50 and AlN. The voltage rise is caused by temperature rise induced by joule heating. Thermal conductivity of DFRP-50 is higher than that of GFRP-50 and lower than that of AlN. Therefore, the difference of the data in the GFRP-50, DFRP-50, and AlN is due to thermal conductivity of the clamping materials and heat transfer from the Bi tape to the clamping materials [38]. It is known that the voltage rise becomes slower by increasing content ratio of DF and contact stress to Bi tape in the case of DFRP [38]. It is considered that the negative thermal expansion of DFRP contributes to increasing contact stress in the HTS coil. The stability of HTS coil is reported in the next section.

3.4. Evaluating Cooling Performance of High-Strength Polyethylene-Fiber-Reinforced Plastics in Conduction-Cooled HTS Coils [8]. In this section, thermal stabilities of HTS coils composed of DFRP, GFRP, and AlN bobbins shown in Figure 18 are reported. DFRP and GFRP bobbins were pipes shown in Figure 19, and those were made by filament winding (FW) method. The specimens of coil and superconductor are shown in Table 2. FW angles of DFRP pipes were 30, 45, and 60 deg. Those are denoted as DFRP60, DFRP30, and DFRP45, respectively. If the angle is larger than 45 degrees, the bobbin expands radially when cooled [36]. When is smaller than 45 degrees, on the other hand, the bobbin contracts when cooled [36]. FW angle of GFRP was 60deg. AlN and GFRP bobbins do not expand when cooled.

The time profiles of voltage tape signals of those coils are shown in Figure 20. Applied current to the HTS coil corresponds to 86A (Ic). The voltage profile of the AlN coil

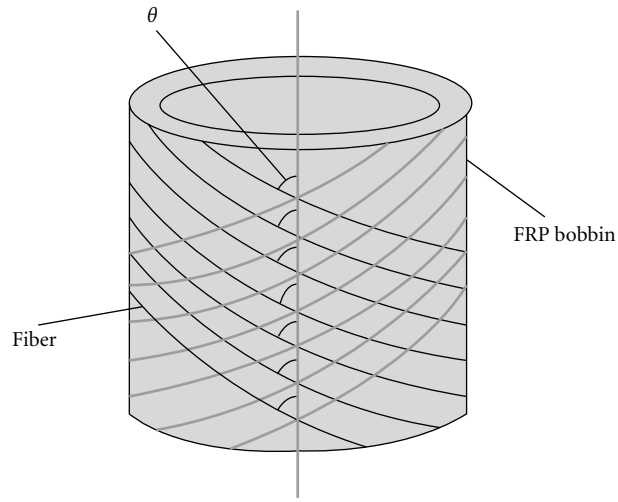

Figure 19: Bobbin shape and fiber angle in bobbin [8].

is almost same as that of the DFRP60 coil even though the thermal conductivity of AlN is more than twice of DFRP60 [56]. The reason is the heat transfer from the tape to the bobbin. The DFRP60 bobbin expanded, and, hence, its heat transfer became better [57]. The AlN bobbin, on the other hand, contracted, and its heat transfer became worse. The thermal conductivity of GFRP is lower than that of the other four materials used in the experiment, and the heat transfer of the GFRP coil is bad because the material contracts when cooled. This is why the measured thermal stability was worst for the coil wound on the GFRP bobbin. Therefore, the thermal stability of the coils depended not only on the thermal conductivity of the bobbin but also on the heat transfer from the tape to the bobbin. Thus, DFRP60 would be a good heat sink material for the bobbin of a conduction-cooled coil [8].

Table 2: Specifications of coil, coil bobbins, and Bi-2223 tapes in the HTS sample coils shown in Figure 19.

Coil and bobbin	Height (mm)	50
	Inner diameter of bobbin (mm)	40
	Outer diameter of bobbin (mm)	55
	Turn/layer	4 turns and single layer
	Winding tension	10 N at room temperature
Conductor	Superconductor	Bi-2223
	Sheath	Silver alloy
	Width (mm)	3.3
	Thickness (mm)	0.7
	Silver ratio	2.2
	Ic at 77 K	86A

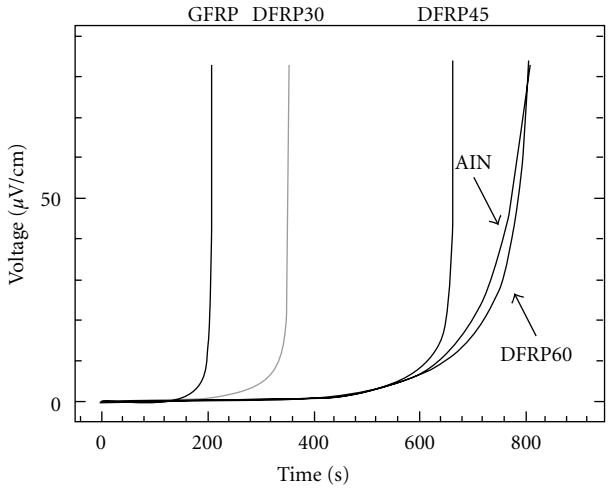

Figure 20: The time profiles of voltage tap signals of HTS coils wound on DFRP, GFRP, and AlN bobbins [8].

References

[1] M. Yoneda and S. Kawabata, "Analysis of transient heat conduction and its application. I. The fundamental analysis and application to thermal conductivity and thermal diffusivity measurements," *Journal of the Textile Machinery Society of Japan*, vol. 34, no. 9, pp. T183–T193, 1981.

[2] M. Yoneda, "Warm/cool feeling in clothing materials," *Journal of the Textile Machinery Society of Japan*, vol. 35, no. 8, pp. P365–P370, 1982.

[3] S. Kawabata, "Developement of a device for measureing heat-moisture transfer properties of apparel fabrics," *Journal of the Textile Machinery Society of Japan*, vol. 37, p. 130, 1984.

[4] S. Nishijima, T. Okada, and K. Niihara, "Design of ceramics with warm feeling," *Key Engineering Materials*, vol. 161–163, pp. 535–538, 1999.

[5] Cryogenic Association of Japan, *Hand Book of Superconductivity and Cryogenic Engineering*, Oumusha, Japan, 1993.

[6] T. Takao, A. Kawasaki, M. Yamaguchi et al., "Investigation of cooling effects on conduction cooled HTS tape due to high thermal conduction plastics," *IEEE Transactions on Applied Superconductivity*, vol. 13, no. 2, pp. 1776–1779, 2003.

[7] C.-M. Ye, B.-Q. Shentu, and Z.-X. Weng, "Thermal conductivity of high density polyethylene filled with graphaite," *Journal of Applied Polymer Science*, vol. 101, pp. 3806–3810, 2006.

[8] T. Takao, T. Yuhara, R. Sakuma, T. Goto, and A. Yamanaka, "Evaluating cooling performance of high-thermal-conduction composite in conduction-cooled superconducting coils," *IEEE Transactions on Applied Superconductivity*, vol. 20, no. 3, pp. 2126–2129, 2010.

[9] T. Bhowmick and S. Pattanayak, "Thermal conductivity, heat capacity and diffusivity of rubbers from 60 to 300 K," *Cryogenics*, vol. 30, no. 2, pp. 116–121, 1990.

[10] M. Jäckel, M. Müller, A. L. Claverie, and K. F. Arndt, "Thermal conductivity of modified epoxy resins with different cross-link densities at low temperatures," *Cryogenics*, vol. 31, no. 4, pp. 228–230, 1991.

[11] C. L. Choy, W. H. Luk, and F. C. Chen, "Thermal conductivity of highly oriented polyethylene," *Polymer*, vol. 19, no. 2, pp. 155–162, 1978.

[12] C. L. Choy, S. P. Wong, and K. Young, "Model calculation of the thermal conductivity of polymer crystals," *Journal of Polymer Science: Polymer Physics Edition*, vol. 23, no. 8, pp. 1495–1504, 1985.

[13] D. B. Mergenthaler, M. Pietralla, S. Roy, and H. G. Killan, "Thermal conductivity in ultraoriented polyethylene," *Macromolecules*, vol. 25, no. 13, pp. 3500–3502, 1992.

[14] S. Burgess and D. Greig, "The low-temperature thermal conductivity of polyethylene," *Journal of Physics C*, vol. 8, no. 11, pp. 1637–1648, 1975.

[15] A. G. Gibson, D. Greig, M. Sahota, I. M. Ward, and C. L. Choy, "Thermal conductivity of ultrahigh-modulus polyethylene," *Journal of Polymer Science: Polymer Letters Edition*, vol. 15, no. 4, pp. 183–192, 1977.

[16] C. L. Choy, "Thermal conductivity of polymers," *Polymer*, vol. 18, no. 10, pp. 984–1004, 1977.

[17] C. L. Choy and W. P. Leung, "Thermal conductivity of ultradrawn polyethylene," *Journal of Polymer Science: Polymer Physics Edition*, vol. 21, no. 7, pp. 1243–1246, 1983.

[18] H. Fujishiro, M. Ikebe, T. Kashima, and A. Yamanaka, "Thermal conductivity and diffusivity of high-strength polymer fibers," *Japanese Journal of Applied Physics, Part 1*, vol. 36, no. 9, pp. 5633–5637, 1997.

[19] H. Fujishiro, M. Ikebe, T. Kashima, and A. Yamanaka, "Drawing effect on thermal properties of high-strength polyethylene fibers," *Japanese Journal of Applied Physics, Part 1*, vol. 37, no. 4, pp. 1994–1995, 1998.

[20] A. Yamanaka, H. Fujishiro, T. Kashima et al., "Thermal conductivity of high strength polyethylene fiber in low temperature," *Journal of Polymer Science, Part B*, vol. 43, no. 12, pp. 1495–1503, 2005.

[21] C. L. Choy, F. C. Chen, and W. H. Luk, "Thermal conductivity of oriented crystalline polymers," *Journal of Polymer Science*, vol. 18, no. 6, pp. 1187–1207, 1980.

[22] C. L. Choy and K. Young, "Thermal conductivity of semicrystalline polymers—a model," *Polymer*, vol. 18, no. 8, pp. 769–776, 1977.

[23] J. Hennig, "Anisotropy and structure in uniaxially stretched amorphous high polymers," *Journal of Polymer Science, Part C*, vol. 16, p. 2751, 1967.

[24] F. H. Müller, "Uniaxial stretching and anisotropy," *Journal of Polymer Science, Part C*, vol. 20, no. 1, pp. 61–76, 1967.

[25] J. Morikawa, J. Tan, and T. Hashimoto, "Study of change in thermal diffusivity of amorphous polymers during glass transition," *Polymer*, vol. 36, no. 23, pp. 4439–4443, 1995.

[26] A. Yamanaka, S. Abe, M. Tsutsumi et al., "Thermal conductivity of ramie fiber drawn in water in low temperature," *Journal of Applied Polymer Science*, vol. 100, no. 3, pp. 2196–2202, 2006.

[27] A. Yamanaka, Y. Izumi, T. Terada et al., "Radiation effect on the thermal conductivity and diffusivity of ramie fibers in a range of low temperatures by γ rays," *Journal of Applied Polymer Science*, vol. 100, no. 6, pp. 5007–5018, 2006.

[28] A. Yamanaka, M. Yoshikawa, S. Abe et al., "Effects of vapor-phase-formaldehyde treatments on thermal conductivity and diffusivity of ramie fibers in the range of low temperature," *Journal of Polymer Science, Part B*, vol. 43, no. 19, pp. 2754–2766, 2005.

[29] http://www.toyobo.co.jp/seihin/dn/dyneema/seihin/koutei.html.

[30] A. Yamanaka, Y. Izumi, T. Kitagawa et al., "The effect of γ-irradiation on thermal strain of high strength polyethylene fiber at low temperature," *Journal of Applied Polymer Science*, vol. 102, no. 1, pp. 204–209, 2006.

[31] S. Abe, M. Tsutsumi, M. Yoshikawa, and Y. Sakaguti, "Effects of water-pretreatment on tensile strength of crosslinked cotton fibers," *Journal of the Textile Machinery Society of Japan*, vol. 53, no. 1, pp. 55–61, 2000.

[32] G. O. Phillips and J. C. Arthur Jr., "Photochemistry and radiation chemistry of cellulose," in *Cellulose Chemistry and Its Applications*, T. P. Nevell and S. H. Zeronian, Eds., chapter 12, p. 290, John Wiley & Sons, New York, NY, USA, 1985.

[33] T. Takao, T. Kashima, and A. Yamanaka, "Mechanical properties: structural composites—influence of sliding directions on frictional properties of GFRPs and DFRPs," *Advances in Cryogenic Engineering*, vol. 46, pp. 119–126, 2000.

[34] T. Nitta, M. Chiba, T. Kashima, and T. Takao, "AC surface spark voltage of pipes composed with high strength polyethylene fiber reinforced plastics in coolant," *Proceedings of MT-15*, vol. 1159, 1998.

[35] T. Okada, S. Nishijima, K. Takahata, and J. Yamamoto, "Research and development of insulating materials for large helical device," *Cryogenics*, vol. 31, no. 4, pp. 307–311, 1991.

[36] T. Kashima, A. Yamanaka, S. Nishijima, and T. Okada, "Thermal strain of pipes composed with high-strength polyethylene fiber reinforced plastics at cryogenic temperatures," *Advances in Cryogenic Engineering*, vol. 42, pp. 147–154, 1996.

[37] S. Abe, M. Yoshikawa, Y. Sakaguchi, and M. Shinjo, "Relation between tensile strength and wash & wear properties of cotton fabrics treated with dihydroxyethyleneurea and vapor-phase-formaldehyde," *Journal of the Textile Machinery Society of Japan*, vol. 52, no. 2, pp. T29–T36, 1999.

[38] T. Takao, A. Watanabe, T. Takiyama, K. Nakamura, and A. Yamanaka, "Heat drain effects from HTS tapes to high thermal conduction plastics for conduction-cooled magnets," *IEEE Transactions on Applied Superconductivity*, vol. 17, no. 2, pp. 2398–2401, 2007.

[39] S. Abe, S. Ohta, and M. Yoshikawa, "Effects of pre-treatments and catalysts-application methods on formaldehyde cross-linking density in cotton fibers finished with vapor-phase-formaldehyde," *Journal of the Textile Machinery Society of Japan*, vol. 50, no. 5, pp. T124–T130, 1997.

[40] S. Abe, S. Ohta, M. Yoshikawa, and M. Tsutsumi, "Effects of pre-treatment on the mechanical and wash & wear properties of cotton fabrics finished with vapor-phase-formaldehyde," *Journal of the Textile Machinery Society of Japan*, vol. 50, no. 6, pp. T139–T145, 1997.

[41] S. Abe, M. Yoshikawa, Y. Shimizu, and Y. Sakaguchi, "Cotton fibers crosslinked by vapor-phase-formaldehyde and dimethyloldihydroxyethyleneurea after pretreatment with liquid ammonia and subsequently: stability to hot water-treatment," *Journal of the Textile Machinery Society of Japan*, vol. 52, no. 12, pp. T274–T281, 1999.

[42] S. M. Stark Jr. and S. P. Rowrand, "Swelling characteristics of gel fractions of formaldehyde-modified cotton celluloses," *Journal of Applied Polymer Science*, vol. 10, no. 11, pp. 1777–1786, 1966.

[43] S. P. Rowland and A. W. Post, "A measure of effective crosslinks in formaldehyde-modified cotton celluloses," *Journal of Applied Polymer Science*, vol. 10, no. 11, pp. 1751–1761, 1966.

[44] G. L. Payet, "ALMI-set process. A new approach to carefree garments," *Textile Research Journal*, vol. 43, no. 4, pp. 194–197, 1973.

[45] S. Abe, S. Ohta, M. Yoshikawa, and M. Tsutsumi, "Effects of pretreatment on the mechanical and wash-and-wear properties of cotton fabrics cross-linked with vapor-phase-formaldehyde and dimethyloldihydroxyethyleneurea," *Journal of the Textile Machinery Society of Japan*, vol. 52, no. 5, pp. T65–T71, 1999.

[46] J. Lemstra, R. Kirschbaum, T. Ohta, and H. Yasuda, "High-strength/high-modulus structures based on flexible macromolecules: gel-spinning and related processes," in *Developments in Oriented Polymers-2*, I. M. Ward, Ed., p. 39, Elsevier, New York, NY, USA, 1987.

[47] P. Smith and P. J. Lemstra, "Ultra-high-strength polyethylene filaments by solution spinning/drawing," *Journal of Materials Science*, vol. 15, no. 2, pp. 505–514, 1980.

[48] Y. Ohta and H. Yasuda, "Progress in gel-spining method—new paradigm for high-performance fibers," *Kobunnshi*, vol. 44, no. 10, p. 658, 1995.

[49] Y. Ohta, "Ultra-high strength polyethylene fiber: properties and applications," *Sen'I Gakkaishi*, vol. 54, no. 1, pp. P8–P11, 1998.

[50] Y. Ohta, "Development of ultra-high-strength, polyetylene fiber 'Dyneema'," *Sen'I Gakkaishi*, vol. 55, no. 12, pp. P413–P417, 1999.

[51] Y. Ohta, "Structural development of ultra-high strength polyethylene fiber during gel-spinning process," *Sen'I Gakkaishi*, vol. 60, no. 9, p. 451, 2004.

[52] Y. Izumi, M. Nishii, T. Seguchi, K. Ema, and T. Yamamoto, "Effect of molecular orientation on the radiolysis of polyethylene in the presence of oxygen," *Radiation Physics and Chemistry*, vol. 37, no. 2, pp. 213–216, 1991.

[53] M. Takeo, S. Sato, M. Matsuo et al., "Dependence on winding tensions for stability of a superconducting coil," *Cryogenics*, vol. 43, no. 10-11, pp. 649–658, 2003.

[54] A. Ishiyama and H. Asai, "A stability criterion for cryocooler-cooled HTS coils," *IEEE Transactions on Applied Superconductivity*, vol. 11, no. 1, pp. 1832–1835, 2001.

[55] Y. Lvovsky, "Conduction crisis and quench dynamics in cryocooler-cooled HTS magnets," *IEEE Transactions on Applied Superconductivity*, vol. 12, no. 1, pp. 1565–1569, 2002.

[56] "TOKUYAMA Co. Ltd.," http://www.shapal.jp/index.html.

[57] N. Sekine, T. Takao, Y. Kojo et al., "Improvement in stability of superconducting coil by different mechanical properties of bobbins," *Physica C*, vol. 392–396, no. 2, pp. 1205–1209, 2003.